Diagn Interv Radiol 2012; 18:344–353

REVIEW

MRI of the lung: state of the art

Mark Wielpütz, Hans-Ulrich Kauczor

ABSTRACT

Magnetic resonance imaging (MRI) of the lung is technically challenging due to the low proton density and fast signal decay of the lung parenchyma itself. Additional challenges consist of tissue loss, hyperinflation, and hypoxic hypoperfusion, e.g., in emphysema, a so-called "minus-pathology". However, pathological changes resulting in an increase of tissue ("plus-pathology"), such as atelectases, nodules, infiltrates, mucus, or pleural effusion, are easily depicted with high diagnostic accuracy. Although MRI is inferior or at best equal to multi-detector computed tomography (MDCT) for the detection of subtle morphological features, MRI now offers an increasing spectrum of functional imaging techniques such as perfusion assessment and measurement of ventilation and respiratory mechanics that are superior to what is possible with MDCT. Without putting patients at risk with ionizing radiation, repeated examinations allow for the evaluation of the course of lung disease and monitoring of the therapeutic response through quantitative imaging, providing a level of functional detail that cannot be obtained by any other single imaging modality. As such, MRI will likely be used for clinical applications beyond morphological imaging for many lung diseases. In this article, we review the technical aspects and protocol suggestions for chest MRI and discuss the role of MRI in the evaluation of nodules and masses, airway disease, respiratory mechanics, ventilation, perfusion and hemodynamics, and pulmonary vasculature.

Key words: • *magnetic resonance imaging* • *lung cancer* • *cystic fibrosis* • *pulmonary arterial hypertension*

From the Department of Diagnostic and Interventional Radiology (H-U.K. ✉ *hu.kauczor@med.uni-heidelberg.de*), Translational Lung Research Center Heidelberg (TLRC-H), Member of the German Center for Lung Research, Heidelberg, Germany.

Received 15 November 2011; accepted 16 November 2011.

Published online 20 March 2012
DOI 10.4261/1305-3825.DIR.5365-11.0

The rationale for using magnetic resonance imaging (MRI) in the management of patients with lung disease is obvious: MRI enables comprehensive structural and functional imaging without ionizing radiation. However, MRI of the lung is extremely challenging for three reasons: 1) the low density tissue of the lung contains a relatively small number of signal-generating protons; 2) the multiple air-tissue interfaces cause substantial susceptibility artifacts which are directly related to a fast decay of signal; and 3) respiratory, vascular, and cardiac motions require fast imaging or time-consuming triggering and gating techniques.

Most lung diseases are associated with an increase in tissue per volume, generally due to the interstitial, alveolar, bronchial or pleural accumulation of cells, extracellular matrix or fluid, which displace air content. Subsequently, these diseases present with an increase of protons as well as a decrease in the air-tissue interfaces, both of which enhance ^{1}H-MRI leading to higher signal (1). Thus, diseases such as atelectases, tumors, effusion, pneumonia, or interstitial lung disease are also referred to as "plus-pathologies".

On the other hand, lung diseases may present with hyperinflation due to obstructive airway disease and emphysematous destruction, e.g., in chronic obstructive pulmonary disease (COPD) or asthma (2). Such changes are regarded as a "minus-pathology" because there is a loss of lung tissue closely related to a loss of blood volume attributable to hypoxic vasoconstriction, also referred to as the Euler-Liljestrand effect. As a result, the degree of hyperinflation has an inverse correlation with the magnetic resonance (MR) signal, which poses additional challenges for MRI (3).

Functional imaging with MRI comprises measurements of perfusion, blood flow, ventilation, gas exchange as well as respiratory motion and mechanics. This versatility is complemented by the non-ionizing nature of the modality, which enables regular surveillance in order to monitor therapy during clinical trials or a regular clinical setting. The combination of morphological and functional lung imaging providing information at high spatial and temporal resolution at the scale of entire organs is a major advantage of MRI and differentiates it from other imaging modalities. In this article, we summarize the current status and the potential future perspectives of MRI in the management of lung disease.

Technical aspects and protocol suggestions

To obtain broad clinical acceptance, MRI of the lung has to be practical, robust, and reproducible. On top of these workflow aspects, MRI has to provide consistently high image quality as well as diagnostic accuracy and a positive therapeutic impact. Different scanner manufacturers provide dedicated protocols for MRI of the lung. A cross-vendor

standard protocol of approximately 15 min in-room time has been recently published by a consensus workgroup (4). This protocol may be customized for particular clinical situations.

For MRI of the lung, standard scanners with a field strength of 1.5 Tesla (T) and full parallel imaging capabilities are recommended (4). Although higher field strength, i.e., 3 T, will theoretically increase the signal to noise ratio, faster signal decay due to susceptibility artifacts poses additional obstacles to lung imaging. Special efforts are needed to obtain similar results at 3 T when compared to 1.5 T, e.g., when imaging nodules (5).

A basic protocol is mainly based on non-contrast breath-holding sequences. During this time, three-dimensional (3D) T1-weighted gradient echo and T2-weighted fast spin echo as well as short tau inversion recovery sequences (STIR) can be used. Respiratory, vascular, and cardiac motions can either be addressed by fast imaging, gating, and triggering techniques, respectively (6). Half-Fourier acquisition or ultra-short echo times are recommended (4). The basic protocol should be extended to contrast-enhanced imaging with high spatial resolution (single-phase MR angiography) or high temporal resolution as in multiphasic MR angiography or perfusion imaging. Complicated and time-consuming sequences requiring respiratory or cardiac gating should be reserved for specific clinical scenarios.

T1-weighted 3D gradient echo sequences, such as a volume interpolated gradient echo sequence, are recommended for the assessment of the mediastinum, pulmonary nodules, masses, and consolidations, and should be repeated with fat saturation after the administration of contrast material (Fig. 1). In COPD, for example, the contrast agent compensates for the decreased signal due to the properties of the "minus-pathology" (Fig. 2).

A T2-weighted fast spin echo half-Fourier acquisition sequence will easily visualize pulmonary infiltrates, inflammatory bronchial wall thickening, as well as mucus and fluid accumulation. Experimental work has shown that the sensitivity of T2-weighted breath-hold or respiratory-gated sequences for infiltrates at least equals that of chest X-ray and multi-detector computed tomography (MDCT) (7). Non-contrast enhanced fast steady state free precession (SSFP) gradient echo sequences, for example, TrueFISP, can display lung vessels with excellent contrast. Thromboembolic material, e.g., in acute pulmonary embolism (PE), will appear as a filling defect with low signal intensity, making this sequence a fast screening method in selected patients (8).

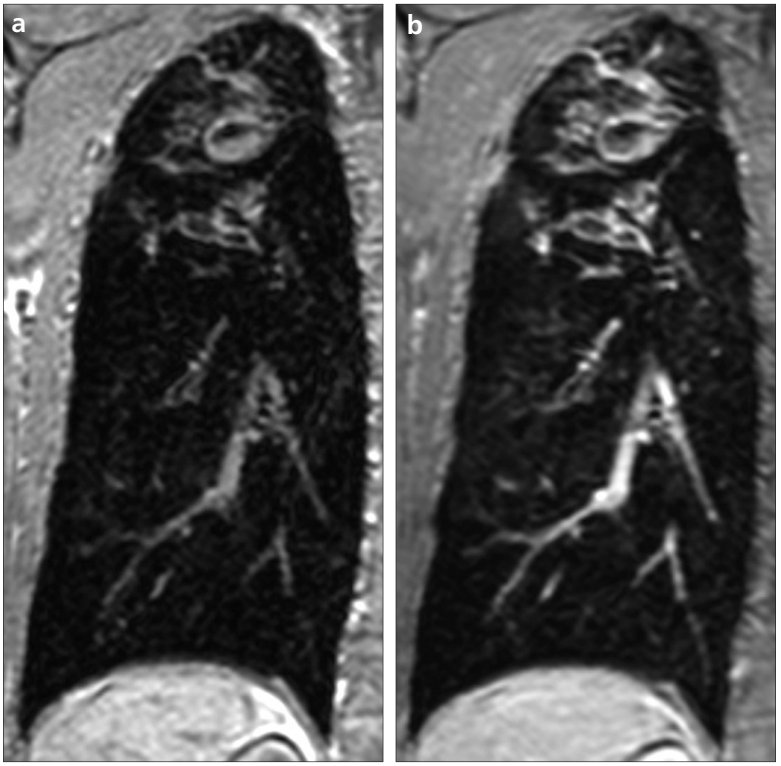

Figure 1. a, b. A 43-year-old patient with cystic fibrosis. Coronal T1-weighted three-dimensional gradient echo sequence **(a)** shows severe bronchiectasis, bronchial wall thickening, and mucus plugging predominantly of the right superior lobe of the lung. The repetition of the sequence after the administration of contrast media **(b)** allows for the differentiation between inflammatory wall thickening and mucus content within bronchi. Courtesy of M. Eichinger and M. Puderbach, Heidelberg Thoracic Imaging Platform, Heidelberg, Germany.

Contrast-enhanced MR perfusion imaging is a straightforward and easy-to-implement technique. Three-dimensional T1-weighted gradient echo sequences with the use of parallel imaging and echo sharing allow for short acquisition times of approximately 1.5 s for a 3D dataset (so-called 4D or 3D + t) needed to visualize perfusion during the peak enhancement of the lung parenchyma. Additionally, high speed acquisition enables time courses in areas with delayed pulmonary arterial perfusion and systemic, broncho-arterial perfusion (Fig. 2) (9). It has been established in nuclear medicine that perfusion defects can also be interpreted as a blueprint of ventilation defects. Due to reflexive hypoxic vasoconstriction, ventilation defects in obstructive pulmonary disease largely correspond to perfusion defects.

For direct ventilation imaging using MRI, several different techniques are available. They either rely on Fourier decomposition (10), "oxygen enhancement" (Fig. 3) (11), or hyperpolarized noble gases (12). MRI after the inhalation of hyperpolarized gases, such as ^{3}He or ^{129}Xe, requires special scanner hardware to image at the respective Larmor frequencies. The complicated handling, high costs in particular for ^{3}He, and the need for the process of laser-induced hyperpolarization at the imaging site have precluded broader clinical application of this technology.

Two-dimensional or 3D dynamic MR techniques, so-called 2D + t and 3D + t, which are based on time-resolved, fast low angle shot or SSFP sequences, can be used to depict the interaction of the chest wall and diaphragm during the respiratory cycle or forced breathing maneuvers at up to 10 frames per second (13). They provide the basis for the analysis of respiratory mechanics.

Figure 2. a–c. Coronal T1-weighted three-dimensional gradient echo sequence **(a)** in a 67-year-old patient with COPD stage IV due to excessive cigarette smoking. Emphysematous areas are hardly resolved due to low signal intensity. The fat saturated contrast-enhanced sequence **(b)** reveals areas of low contrast uptake corresponding to extensive emphysema, predominantly of the lower lobes in this patient. MRI perfusion imaging **(c)** confirms large perfusion defects of the right upper and both lower lungs. Due to hypoxic vasoconstriction, perfusion can be regarded as a blueprint of ventilation. Courtesy of A. Anjorin, Heidelberg Thoracic Imaging Platform, Heidelberg, Germany.

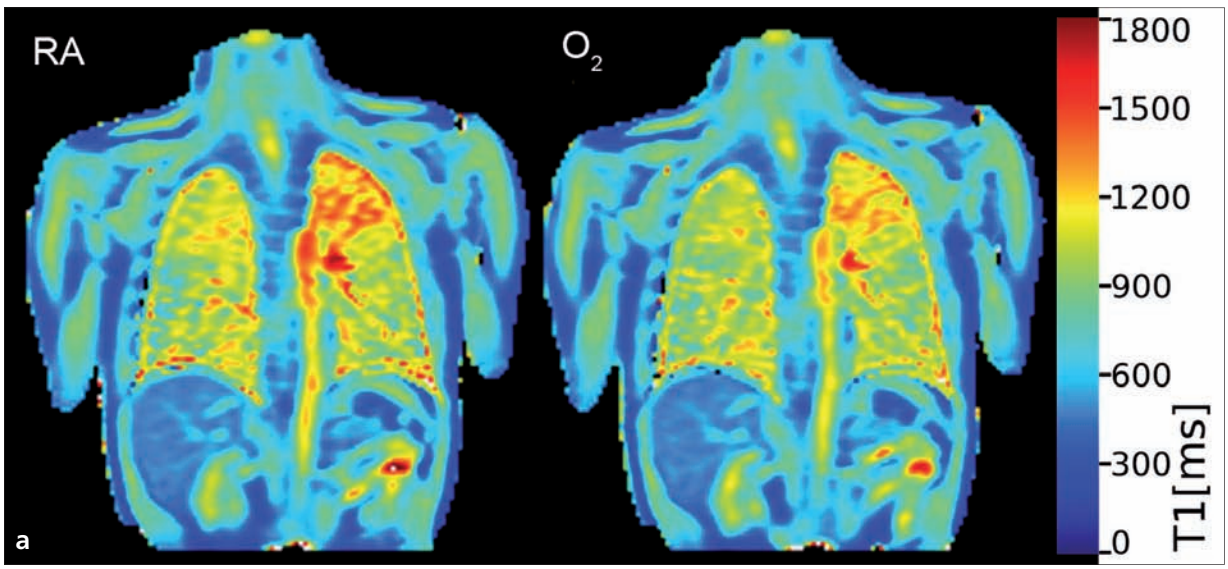

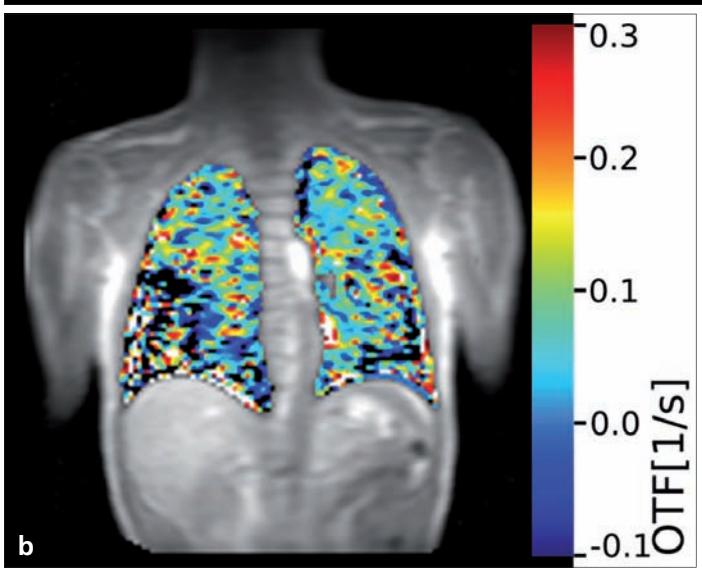

Figure 3. a, b. Further imaging of the patient from Fig. 2. The two maps **(a)** display the T1 relaxation time while breathing room air (RA) (left image) and after 15 L of pure oxygen (O_2) over 10 min (right image). The latter shows a shortening of T1 predominantly in the left upper lobe after O_2 administration. The subtraction of both datasets **(b)** allows for the quantification of the oxygen transfer factor (OTF), which is a result of ventilation, perfusion, and diffusion. The areas of reduced OTF correspond well with perfusion defects in this patient (Fig. 2c). Courtesy of S. Triphan, Institute of Physics, University of Wuerzburg, Germany.

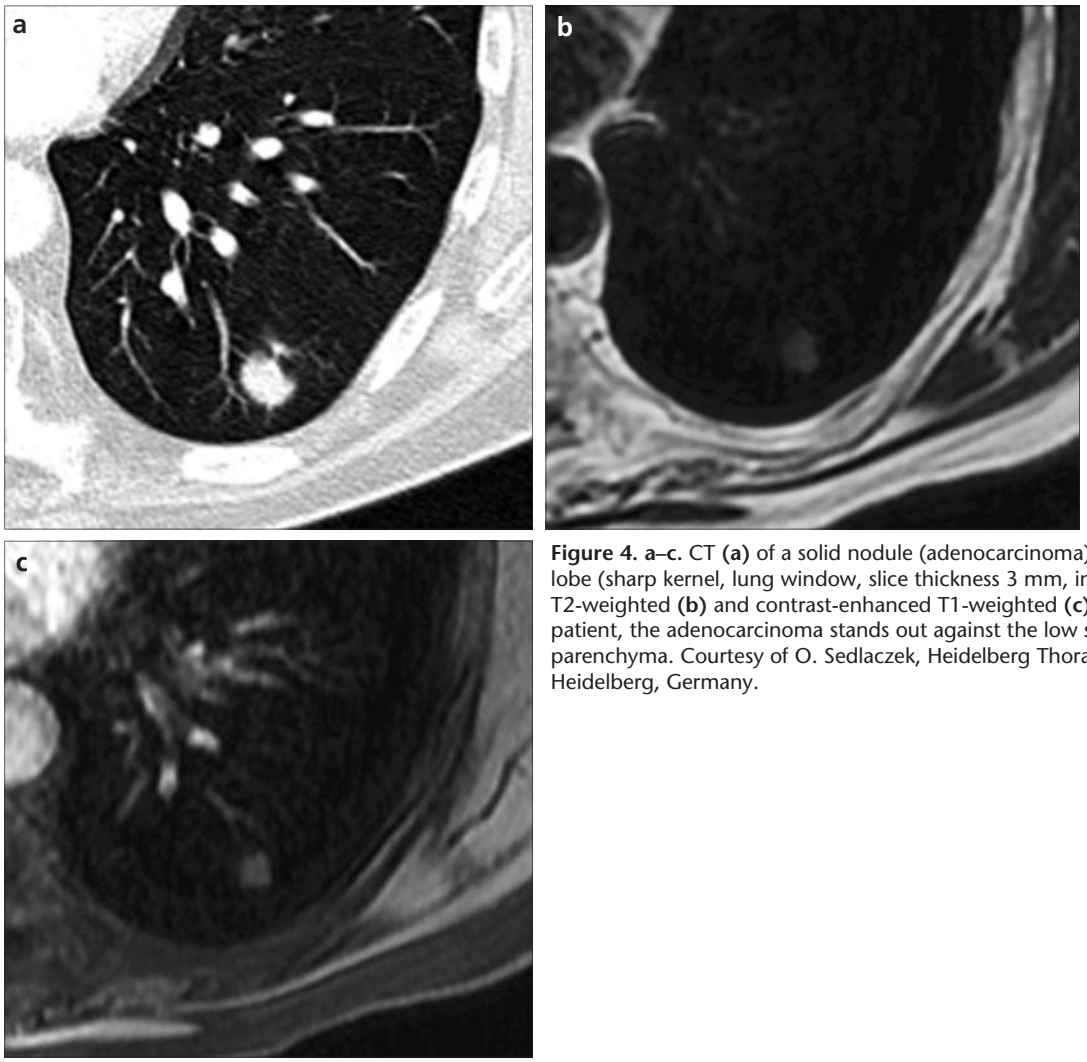

Figure 4. a–c. CT **(a)** of a solid nodule (adenocarcinoma) within the left inferior lobe (sharp kernel, lung window, slice thickness 3 mm, increment 2 mm). On the T2-weighted **(b)** and contrast-enhanced T1-weighted **(c)** sequences of the same patient, the adenocarcinoma stands out against the low signal intensity of the lung parenchyma. Courtesy of O. Sedlaczek, Heidelberg Thoracic Imaging Platform, Heidelberg, Germany.

MRI in the management of pulmonary diseases

Currently, there are some first-line indications for MRI of the lung, mainly in the pediatric population. These include cardio-pulmonary vascular anomalies, such as pulmonary arteriovenous malformations, pulmonary sequestration, pulmonary artery hypoplasia, partial or total anomalous pulmonary venous return, persistent left superior vena cava, or pulmonary artery sling. In addition, MRI may be indicated for bronchopulmonary dysplasia, cystic fibrosis (CF), and pectus excavatum. Lung cancer of the superior sulcus, the so-called Pancoast tumor, is another important indication for MRI in adults. We also propose some additional lung diseases, which—after a chest X-ray—should have a further imaging work-up by MRI of the lung: pulmonary arterial hypertension (PAH) and non-small cell lung cancer when differentiation between resectability (T3) and non-resectability (T4) is critical. This is especially so with regard to detecting infiltration of the chest wall, diaphragm, or mediastinum.

In other lung diseases, MRI will only serve as a second-line cross-sectional imaging modality, e.g., if there are contraindications to iodine or radiation exposure, or as a problem-solving tool if MDCT was inconclusive or results from MDCT and other diagnostic tests, such as scintigraphy or bronchoscopy, are contradictory. These may also include PE and lung cancer staging in general.

Nodules and masses

Nodule detection, characterization and lung cancer staging provide a major workload for MDCT scanners in many centers. For curative resection of lung cancer, imaging methods have to provide reliable information on the local (T stage), lymphatic (N stage), and hematogeneous spread (M stage). Complementary nuclear medicine techniques are employed in the workup of lung cancer patients: a combination of positron emission tomography with computed tomography (PET/CT), as well as bone, ventilation, or perfusion scintigraphy. Recent work suggest the possibility that a comprehensive MR examination (lung and whole body) can provide all the required information in certain lung tumor patients and might have the potential to substitute for MDCT and nuclear medicine examinations in the future (a "one-stop shop").

Under optimal conditions, a threshold size for the detection of pulmonary nodules of approximately 3–4 mm can be obtained by MRI with a sensitivity of 80% to 90%. Sensitivity reaches 100% for lesions larger than

8 mm (1, 4). Multiple sequence types have been suggested for lung nodule detection, e.g., T2-weighted fast spin-echo imaging with and without fat saturation (14), inversion recovery sequences (15), T1-spin echo and gradient echo sequences (16), or a combination thereof that maximizes diagnostic accuracy. Because the normal lung has relatively low background signal, nodules tend to stand out with strong contrast against the dark lung parenchyma, making nodule detection with MRI possibly more efficient than with MDCT (Fig. 4). Additional T1-weighted sequences with fat saturation after contrast administration are recommended to differentiate nodules and vascular lesions. T2-weighted or STIR sequences are recommended to detect infiltrates, lesions with high fluid content, and mediastinal lymph nodes. Tumor heterogeneity, such as with necrotic components, is clearly visualized in contrast-enhanced sequences, and might influence therapy planning and prognosis. In this context, diffusion-weighted imaging (DWI) might also be helpful to differentiate post-stenotic atelectasis from the underlying central mass.

In cancer of the superior sulcus (Pancoast tumor), MRI is mandatory to delineate tumor infiltration of the chest wall and especially the brachial plexus and vasculature, all of which strongly influence resectability, resection margins, and the gross tumor volume for radiotherapy. Furthermore, in many patients, the differentiation between T3 and T4 stages is critical for referral to surgical treatment. Several studies relying on contrast-enhanced MR angiography and cardiac-gated sequences could show advantages of MRI over MDCT in the assessment of cardiovascular or mediastinal invasion (17). Another simple method to assess mediastinal as well as thoracic wall infiltration constitutes the use of time-resolved steady state sequences acquired dynamically in free-breathing (18).

In assessing the progression of cancer to the N stage, the detection of contralateral mediastinal or hilar lymph node involvement is of utmost importance, as it will exclude these patients from surgical treatment. The most accepted morphological criterion for a positive finding on MDCT, the standard imaging modality for lung cancer staging is size, specifically, if the tumor is >10 mm in the short axis or >15 mm in the long axis. As such, the accuracy of morphological lymph node evaluation by MDCT is extremely limited, with a sensitivity and specificity as low as 52% and 69%, respectively (19). Using the conventional morphologic criteria for lymph node assessment, MRI is inferior to MDCT because benign calcifications are not distinguished from metastatic growth. Recently, cardiac—and/or respiratory—triggered STIR sequences have been introduced into mediastinal lymph node assessment, which allows imaging of metastatic lymph nodes with high signal intensity and also allows for the quantification of signal intensity relative to a saline phantom (20). Reports on sensitivity and specificity on a per-patient basis range between 84% and 100% as well as 75% and 93%, respectively (20, 21). Thus, MRI with STIR imaging should be discussed as an alternative to fluorodeoxyglucose (FDG) PET/CT for lymph node assessment (20). The use of DWI in the assessment of masses or lymph node involvement is still subject to evaluation, but has also shown promising results for whole-body staging of lung cancer (22).

The main target sites of lung cancer metastasis (M stage) are the adrenal glands, brain, and bone. MRI proves superior accuracy in the individual evaluation of these organ systems, which cannot be covered by this review in detail. However, whole-body MRI with modern fast techniques has been suggested as a diagnostic tool for M staging, which can be implemented into a comprehensive lung cancer staging protocol. This technique has already proved to sensitively detect extrathoracic spread. A direct comparison between whole-body MRI and FDG PET/CT has shown that whole-body MRI has significantly higher sensitivity for metastatic disease, mainly owing to a higher accuracy in determining the degree of brain, neck, and bone involvement (23).

Airway disease

Parenchymal findings

MRI of airway diseases such as COPD, CF lung disease, and asthma has been a central focus of MRI research for many years. Previously, this has resulted in the introduction of lung MRI into the routine clinical management of CF in many centers.

COPD may present with different etiologies: 1) the airway-type, which is usually related to chronic bronchitis and low to moderate airflow obstruction and 2) the emphysema-type, which is related to the destruction of the lung parenchyma with distal airspace enlargement and severe airflow obstruction (2). The latter is a "minus-pathology" due to the loss of tissue. Since the signal is greatly reduced, the emphysema itself is difficult to diagnose by structural ^{1}H-MRI (24) (Fig. 2).

Compared with COPD, CF lung disease can be considered a "plus-pathology" due to bronchial wall thickening, bronchial dilatation, and mucus plugging (25), which are easily identified with MRI (Figs. 1a and 5a). In addition, MRI can also highlight inflammatory wall changes, including edema and intraluminal mucus due to different signal properties on T1- and T2-weighted images as well as pre- and postcontrast. Wall inflammation demonstrates an obvious contrast enhancement, whereas mucus plugging is especially well visualized by MRI because of the high T2 signal of the fluid content, but without contrast enhancement (Fig. 1b). Peripheral mucus plugging shows a grapelike appearance of small T2-weighted high intensity areas, similar to the ''tree-in-bud'' pattern in computed tomography (CT), thus visualizing small airways with MRI (Fig. 5a). In other "plus-pathologies", such as cavitations or sacculations with air-fluid levels, consolidations, and segmental/lobar destructions MRI is also clearly comparable to CT (2). Thus, MRI has been shown to be equivalent to MDCT in manifest CF in patients older than six years (26). However, comprehensive functional MRI may have additional future clinical impact beyond that of simple morphologic imaging in airway disease.

Respiratory mechanics

Hyperinflation of the lung in COPD severely affects respiratory mechanics and is associated with increased elastic recoil. In contrast to the normal synchronous motion of the diaphragm and chest wall, patients with emphysema will show a pattern of reduced, irregular, or asynchronous motion (27).

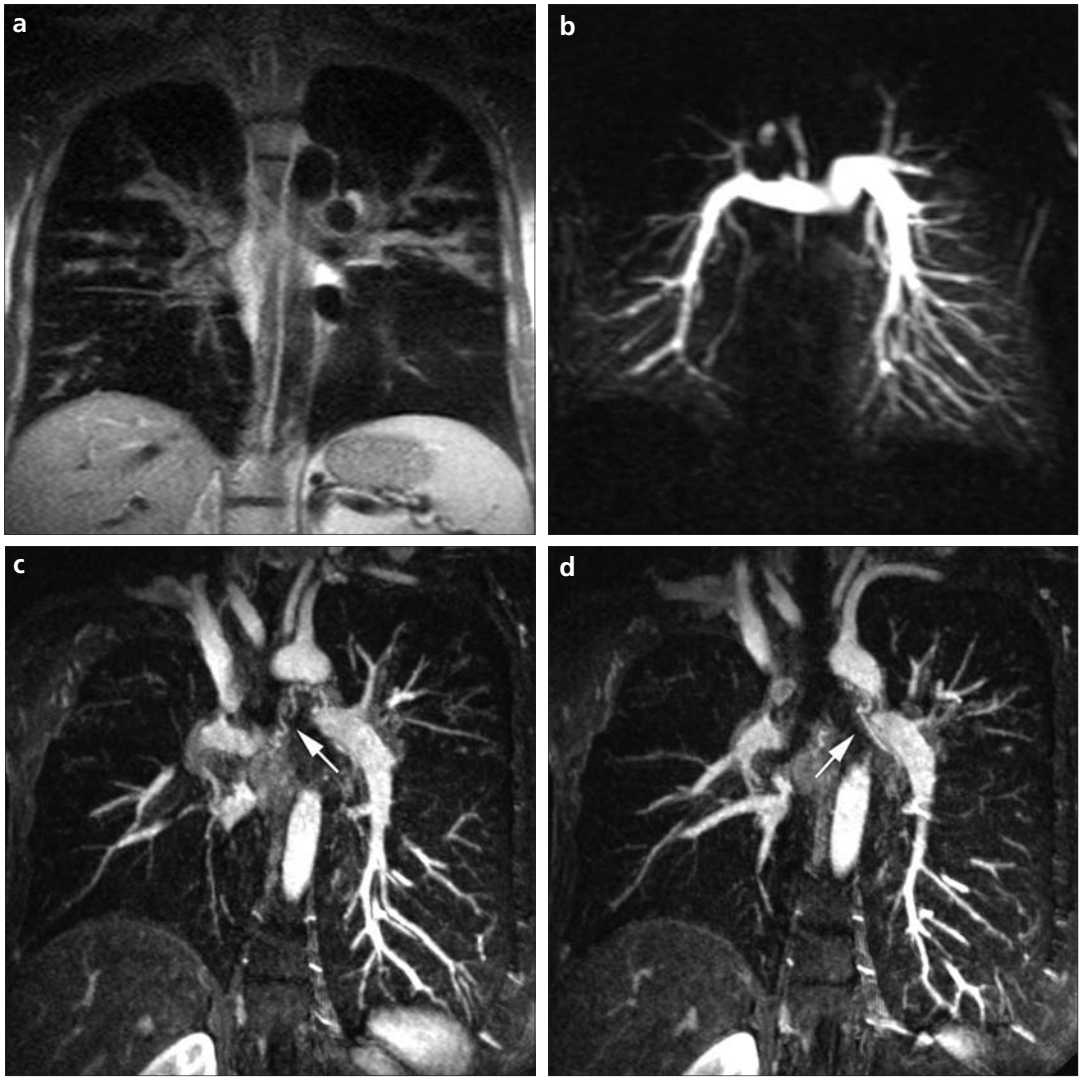

Figure 5. a–d. The coronal T2-weighted fast spin echo half-Fourier acquisition sequence **(a)** depicts severe wall-thickening and mucus plugging from lobar to distal bronchi in a 31-year-old patient with cystic fibrosis. Peripheral mucus plugging shows a grape-like appearance similar to the tree-in-bud phenomenon known from CT (left superior lobe, right inferior lobe). MR perfusion imaging **(b)** reveals extensive perfusion defects of both superior lungs (coronal maximum intensity projection [MIP], slice thickness 20 mm). Within the same examination, an MR angiography was acquired, which demonstrated dilated bronchial arteries (*white arrows*) to the right **(c)** and left lung **(d)** (double angulated MIP, slice thickness 10 mm). Courtesy of M. Puderbach, M. Eichinger and D. E. Optazaite, Heidelberg Thoracic Imaging Platform, Heidelberg, Germany.

This can be readily visualized by dynamic MRI with all the advantages of a cross-sectional imaging method when compared to fluoroscopy. Further developments in MRI should allow for a reliable and regional analysis of lung function that cannot be obtained by pulmonary function tests.

Ventilation

The clinical application of ventilation MRI in COPD patients is challenging. Oxygen-enhanced MRI will show a significantly lower increase in signal after inhalation of pure oxygen and an inhomogeneous distribution pattern. Ohno et al. (28) demonstrated that these regional changes at oxygen-enhanced MRI correspond to regional lung function.

Hyperpolarized ^{3}He-MRI has been used extensively in asthmatic patients for detecting ventilation defects, which were distributed throughout the lungs. These ventilation defects were more numerous and larger in patients with symptomatic asthma and abnormal spirometry than in asymptomatic patients. The distribution of ventilation defects shows that many ventilation defects persisted or recurred in the same location over repeated bronchoconstriction events. This suggests that the regional changes of airflow obstruction are relatively fixed within the lung (29).

Perfusion and hemodynamics

Air-trapping and hyperinflation lead to reflectory hypoxic vasoconstriction, but COPD is also thought to directly affect the pulmonary arteries, with chronic inflammation leading to intimal wall thickening and smooth muscle hypertrophy. Furthermore, parenchymal destruction goes along with destruction of the pulmonary vascular bed. Still, the distribution of perfusion does not necessarily match parenchymal destruction (30).

MR perfusion has already demonstrated a high diagnostic accuracy in detecting perfusion abnormalities in patients suffering from emphysema (31) as well as good agreement with the gold standard, radionuclide perfusion scintigraphy (32). The perfusion abnormalities in COPD (Fig. 2c) differ clearly from those caused by vascular occlusion. Although in embolic obstruction similar wedge-shaped perfusion defects occur, generally a low degree of contrast enhancement is found in COPD patients, especially those with severe emphysema (33). Furthermore, the peak signal intensity of the lung parenchyma after contrast administration is reduced. These features allow for easy visual differentiation.

Figure 6. a–e. A comprehensive diagnostic work-up by MRI in acute pulmonary embolism. A 20-year-old female patient underwent contrast-enhanced MDCT **(a)** for suspected pulmonary embolism, and central as well as peripheral clots were detected. A coronal steady-state free precession sequence of free breathing **(b)** depicts central emboli without necessity for contrast media. The contrast-enhanced MR angiography **(c)** shows the corresponding filling defects. Additionally, MR perfusion imaging **(d)** reveals extensive perfusion defects due to thromboembolic occlusion. Bilateral infarction pneumonia is depicted by fast spin echo T2-weighted sequences in this patient **(e)**.

In children with CF, perfusion defects imaged with MRI (Fig. 5b) correlated with the degree of tissue destruction (34). It seems reasonable that the reversibility of perfusion defects after a therapeutic intervention might serve as an indicator for response to therapy as well as a means to differentiate between regions with reversible and irreversible disease. In CF, dilatation of bronchial arteries is frequently observed (Fig. 5c and 5d). A higher flow in the bronchial arteries leads to a shunt volume from the systemic into the pulmonary circulation, which can be assessed by MRI-based flow measurements. Decreased peak blood flow velocities in the pulmonary arteries were found in 10 patients who had CF compared with 15 healthy volunteers. This may represent the early development of pulmonary hypertension in this patient group (30).

Pulmonary vasculature

As discussed previously, non-enhanced as well as contrast-enhanced techniques are readily available to study pulmonary vasculature and perfusion. The most obvious candidates for vascular MRI are children with suspected congenital vascular abnormalities. These rare but often severe conditions are first-line indications for MRI, but cannot be thoroughly covered by this review, and has been discussed at length in the existing literature. Other important candidates for MRI are patients suspected of PE when radiation exposure is contraindicated, i.e., pregnant women. SSFP sequences acquired in free breathing show emboli as dark clots against bright vessels (Fig. 6) and allow for fast screening with a sensitivity of more than 90% for central and up to 80% for segmental emboli (8, 35). Thus, exams for PE should be started with SSFP sequences in three planes, and in many cases the exam can be concluded after this point when findings are positive for PE. The examination time is as low as for the gold standard, MDCT, which is beneficial for instable patients.

The highest spatial resolution detection of peripheral emboli is currently achieved by MR angiography with T1-weighted 3D gradient echo breath hold acquisitions using a contrast power injector. The recent multicenter PIOPED III study demonstrated a sensitivity and specificity for acute PE of 78% and 99%, respectively (36). Under study conditions, sufficient image quality was achieved in 75% of patients only, mainly due to dyspnea, coughing, and faulty contrast timing. These obstacles can partially be obviated by time-resolved MR perfusion imaging at the cost of some spatial resolution. With this technique, a sensitivity of 98% for lobar and 92% for segmental PE has been achieved (37). In a comparative study, a combination of SSFP, contrast-enhanced MR angiography, and MR perfusion imaging yielded the best sensitivity and specificity (8). A combined approach may also partially reduce the high risk of non-diagnostic scans. In summary, MRI is not yet the method of choice for PE in general but is reserved for cases when ionizing radiation or iodinated contrast agents are contraindicated.

PAH is a condition for which MRI can be extremely beneficial. PAH may present as idiopathic PAH or in association with a plentitude of pulmonary, vascular, and collagen-vascular diseases. PAH is defined as an elevation of the mean pulmonary arterial pressure above 25 mmHg, measured by invasive right heart catheterization. From the radiologist's point of view, MRI can prove useful in identifying conditions leading to PAH and detect changes secondary to PAH in the lung parenchyma, pulmonary arteries, and heart function (38). Quantitative read-outs of pulmonary perfusion have been established using different techniques. The most robust is the measurement of the mean transit time derived from time-resolved contrast-enhanced 3D perfusion datasets, which can be complemented by the model-based calculation of pulmonary blood flow and blood volume. Compared to healthy volunteers, patients with PAH show significantly decreased the mean transit time, pulmonary blood flow and blood volume, and a heterogeneous distribution (39). The assessment of pulmonary arterial blood flow and right ventricular function can be performed by phase contrast flow measurements in the pulmonary trunk or by short axis cine-acquisition of the right ventricle (40). Changes of the complex geometry of the right ventricular wall and the end-diastolic volume of the right ventricle can be accurately measured with MRI, a useful indicator because right ventricular hypertrophy is one of the earliest signs of right ventricular pressure increase (40).

Chronic thromboembolic pulmonary hypertension (CTEPH) can be found even in patients without a history of prior PE or deep vein thrombosis (41), and may co-exist with other lung diseases such as COPD. The reported incidence of CTEPH two years after diagnosed PE is 3.8% (42). Based on these data, MR perfusion imaging has proved useful as a follow-up tool to document thrombolysis after appropriate treatment (43). If thrombolysis does not occur, the material will be organized and the lumen recanalized in a chronic process, leaving characteristic webs and bands, pouch-like endings of arteries and stenoses (44). If more than 60% of the total arterial diameter becomes obstructed, the patient will develop symptoms of PAH. Contrast-enhanced MR angiography can depict typical CTEPH-related findings of the pulmonary arterial tree down to the segmental level with equal accuracy compared to the gold standard, invasive pulmonary digital subtraction angiography (70). MRI was also superior in defining the exact central beginning of the thromboembolic material (45), a prerequisite for surgical thrombendarterectomy (44). As in acute PE, complementary MR perfusion should be performed to identify typical wedge-shaped perfusion defects, as opposed to patchy or diffuse defects in idiopathic PAH (46).

Conclusion

MRI has been developed into a first-line imaging method in some pulmonary diseases such as congenital cardio-pulmo-vascular anomalies, bronchopulmonary dysplasia, CF, pectus excavatum, and Pancoast tumors. MRI can be of added value in patients with locally or systemically advanced lung cancer when the decision for surgery is critical. Whole-body MRI also has the potential to replace more invasive diagnostic procedures in a lung cancer work-up. Much work has been performed on COPD and CF, and functional techniques are readily transferable to other lung conditions, such as interstitial lung diseases. When ionizing radiation or iodinated contrast agents are contraindicated, MRI

can provide a valuable alternative to MDCT, for example in the detection of acute PE. For the same reason, MRI is a powerful tool for the surveillance of lung disease and monitoring of therapy. MRI has been developed to comprehensively image characteristic changes of the diseased lung, their functional precursors and the consequences at the level of perfusion, ventilation, and respiratory mechanics. Having moved beyond the research stage, pulmonary MRI has now become a practical tool ready to be used in every day clinical routine.

Conflict of interest disclosure

H-U. Kauczor is a member of an advisory board on MRI of the lung with Siemens Healthcare. M. Wielpütz declared no conflicts of interest.

References

1. Biederer J, Hintze C, Fabel M. MRI of pulmonary nodules: technique and diagnostic value. Cancer Imaging 2008; 8:125–130.
2. Ley-Zaporozhan J, Puderbach M, Kauczor HU. MR for the evaluation of obstructive pulmonary disease. Magn Reson Imaging Clin N Am 2008; 16:291–308.
3. Iwasawa T, Takahashi H, Ogura T, et al. Correlation of lung parenchymal MR signal intensity with pulmonary function tests and quantitative computed tomography (CT) evaluation: a pilot study. J Magn Reson Imaging 2007; 26:1530–1536.
4. Biederer J, Beer M, Hirsch W, et al. MRI of the Lung (2/3): Why ... when ... how? Insights Imaging 2011; In press. DOI 10.1007/s13244-011-0146-8
5. Fink C, Puderbach M, Biederer J, et al. Lung MRI at 1.5 and 3 Tesla: observer preference study and lesion contrast using five different pulse sequences. Invest Radiol 2007; 42:377–383.
6. Puderbach M, Hintze C, Ley S, Eichinger M, Kauczor HU, Biederer J. MR imaging of the chest: a practical approach at 1.5T. Eur J Radiol 2007; 64:345–355.
7. Biederer J, Busse I, Grimm J, et al. Sensitivity of MRI in detecting alveolar Infiltrates: Experimental studies. Rofo 2002; 174:1033–1039.
8. Kluge A, Luboldt W, Bachmann G. Acute pulmonary embolism to the subsegmental level: diagnostic accuracy of three MRI techniques compared with 16-MDCT. AJR Am J Roentgenol 2006; 187:7–14.
9. Fink C, Puderbach M, Bock M, et al. Regional lung perfusion: assessment with partially parallel three-dimensional MR imaging. Radiology 2004; 231:175–184.
10. Bauman G, Lutzen U, Ullrich M, et al. Pulmonary functional imaging: qualitative comparison of Fourier decomposition MR imaging with SPECT/CT in porcine lung. Radiology 2011; 260:551–559.
11. Ley S, Puderbach M, Risse F, et al. Impact of oxygen inhalation on the pulmonary circulation: assessment by magnetic resonance (MR)-perfusion and MR-flow measurements. Invest Radiol 2007; 42:283–290.
12. van Beek EJ, Wild JM, Kauczor HU, Schreiber W, Mugler JP 3rd, de Lange EE. Functional MRI of the lung using hyperpolarized 3-helium gas. J Magn Reson Imaging 2004; 20:540–554.
13. Plathow C, Fink C, Ley S, et al. Measurement of diaphragmatic length during the breathing cycle by dynamic MRI: comparison between healthy adults and patients with an intrathoracic tumor. Eur Radiol 2004; 14:1392–1399.
14. Regier M, Kandel S, Kaul MG, et al. Detection of small pulmonary nodules in high-field MR at 3 T: evaluation of different pulse sequences using porcine lung explants. Eur Radiol 2007; 17:1341–1351.
15. Baumann T, Ludwig U, Pache G, et al. Detection of pulmonary nodules with move-during-scan magnetic resonance imaging using a free-breathing turbo inversion recovery magnitude sequence. Invest Radiol 2008; 43:359–367.
16. Biederer J, Both M, Graessner J, et al. Lung morphology: fast MR imaging assessment with a volumetric interpolated breath-hold technique: initial experience with patients. Radiology 2003; 226:242–249.
17. Ohno Y, Adachi S, Motoyama A, et al. Multiphase ECG-triggered 3D contrast-enhanced MR angiography: utility for evaluation of hilar and mediastinal invasion of bronchogenic carcinoma. J Magn Reson Imaging 2001; 13:215–224.
18. Seo JS, Kim YJ, Choi BW, Choe KO. Usefulness of magnetic resonance imaging for evaluation of cardiovascular invasion: evaluation of sliding motion between thoracic mass and adjacent structures on cine MR images. J Magn Reson Imaging 2005; 22:234–241.
19. Webb WR, Gatsonis C, Zerhouni EA, et al. CT and MR imaging in staging non-small cell bronchogenic carcinoma: report of the Radiologic Diagnostic Oncology Group. Radiology 1991; 178:705–713.
20. Ohno Y, Koyama H, Nogami M, et al. STIR turbo SE MR imaging vs. coregistered FDG-PET/CT: quantitative and qualitative assessment of N-stage in non-small-cell lung cancer patients. J Magn Reson Imaging 2007; 26:1071–1080.
21. Ohno Y, Hatabu H, Takenaka D, et al. Metastases in mediastinal and hilar lymph nodes in patients with non-small cell lung cancer: quantitative and qualitative assessment with STIR turbo spin-echo MR imaging. Radiology 2004; 231:872–879.
22. Chen W, Jian W, Li HT, et al. Whole-body diffusion-weighted imaging vs. FDG-PET for the detection of non-small-cell lung cancer. How do they measure up? Magn Reson Imaging 2010; 28:613–620.
23. Ohno Y, Koyama H, Nogami M, et al. Whole-body MR imaging vs. FDG-PET: comparison of accuracy of M-stage diagnosis for lung cancer patients. J Magn Reson Imaging 2007; 26:498–509.
24. Ley-Zaporozhan J, Ley S, Eberhardt R, Kauczor HU, Heussel CP. Visualization of morphological parenchymal changes in emphysema: comparison of different MRI sequences to 3D-HRCT. Eur J Radiol 2010; 73:43–49.
25. Eichinger M, Heussel CP, Kauczor HU, Tiddens H, Puderbach M. Computed tomography and magnetic resonance imaging in cystic fibrosis lung disease. J Magn Reson Imaging 2010; 32:1370–1378.
26. Puderbach M, Eichinger M, Haeselbarth J, et al. Assessment of morphological MRI for pulmonary changes in cystic fibrosis (CF) patients: comparison to thin-section CT and chest x-ray. Invest Radiol 2007; 42:715–725.
27. Suga K, Tsukuda T, Awaya H, et al. Impaired respiratory mechanics in pulmonary emphysema: evaluation with dynamic breathing MRI. J Magn Reson Imaging 1999; 10:510–520.
28. Ohno Y, Sugimura K, Hatabu H. Clinical oxygen-enhanced magnetic resonance imaging of the lung. Top Magn Reson Imaging 2003; 14:237–243.
29. de Lange EE, Altes TA, Patrie JT, et al. The variability of regional airflow obstruction within the lungs of patients with asthma: assessment with hyperpolarized helium-3 magnetic resonance imaging. J Allergy Clin Immunol 2007; 119:1072–1078.
30. Ley S, Puderbach M, Fink C, et al. Assessment of hemodynamic changes in the systemic and pulmonary arterial circulation in patients with cystic fibrosis using phase-contrast MRI. Eur Radiol 2005; 15:1575–1580.
31. Sergiacomi G, Sodani G, Fabiano S, et al. MRI lung perfusion 2D dynamic breath-hold technique in patients with severe emphysema. In Vivo 2003; 17:319–324.
32. Molinari F, Fink C, Risse F, Tuengerthal S, Bonomo L, Kauczor HU. Assessment of differential pulmonary blood flow using perfusion magnetic resonance imaging: comparison with radionuclide perfusion scintigraphy. Invest Radiol 2006; 41:624–630.
33. Morino S, Toba T, Araki M, et al. Noninvasive assessment of pulmonary emphysema using dynamic contrast-enhanced magnetic resonance imaging. Exp Lung Res 2006; 32:55–67.
34. Eichinger M, Puderbach M, Fink C, et al. Contrast-enhanced 3D MRI of lung perfusion in children with cystic fibrosis--initial results. Eur Radiol 2006; 16:2147–2152.
35. Kluge A, Muller C, Hansel J, Gerriets T, Bachmann G. Real-time MR with TrueFISP for the detection of acute pulmonary embolism: initial clinical experience. Eur Radiol 2004; 14:709–718.
36. Stein PD, Chenevert TL, Fowler SE, et al. Gadolinium-enhanced magnetic resonance angiography for pulmonary embolism: a multicenter prospective study (PIOPED III). Ann Intern Med 2010; 152:434–443.

37. Ersoy H, Goldhaber SZ, Cai T, et al. Time-resolved MR angiography: a primary screening examination of patients with suspected pulmonary embolism and contraindications to administration of iodinated contrast material. AJR Am J Roentgenol 2007; 188:1246–1254.
38. Nagendran J, Michelakis E. MRI: one-stop shop for the comprehensive assessment of pulmonary arterial hypertension? Chest 2007; 132:2–5.
39. Ley S, Mereles D, Risse F, et al. Quantitative 3D pulmonary MR-perfusion in patients with pulmonary arterial hypertension: correlation with invasive pressure measurements. Eur J Radiol 2007; 61:251–255.
40. Vonk-Noordegraaf A, Marcus JT, Holverda S, Roseboom B, Postmus PE. Early changes of cardiac structure and function in COPD patients with mild hypoxemia. Chest 2005; 127:1898–1903.
41. Peacock A, Simonneau G, Rubin L. Controversies, uncertainties and future research on the treatment of chronic thromboembolic pulmonary hypertension. Proc Am Thorac Soc 2006; 3:608–614.
42. Pengo V, Lensing AW, Prins MH, et al. Incidence of chronic thromboembolic pulmonary hypertension after pulmonary embolism. N Engl J Med 2004; 350:2257–2264.
43. Kluge A, Gerriets T, Lange U, Bachman G. MRI for short-term follow-up of acute pulmonary embolism. Assessment of thrombus appearance and pulmonary perfusion: a feasibility study. Eur Radiol 2005; 15:1969–1977.
44. Dartevelle P, Fadel E, Mussot S, et al. Chronic thromboembolic pulmonary hypertension. Eur Respir J 2004; 23:637–648.
45. Kreitner KF, Ley S, Kauczor HU, et al. Chronic thromboembolic pulmonary hypertension: pre- and postoperative assessment with breath-hold MR imaging techniques. Radiology 2004; 232:535–543.
46. Ley S, Fink C, Zaporozhan J, et al. Value of high spatial and high temporal resolution magnetic resonance angiography for differentiation between idiopathic and thromboembolic pulmonary hypertension: initial results. Eur Radiol 2005; 15:2256–2263.